Secular and Multidecadal Warming of the Atlantic Ocean since the mid-20th Century

Sang-Ki Lee[1,2], David B. Enfield[1,2], Wonsun Park[3], Erik van Sebille[5], Chunzai Wang[2], Steven Yeager[4], Ben Kirtman[5], and Molly Baringer[2]

[1]Cooperative Institute for Marine and Atmospheric Studies, University of Miami, Miami, Florida, USA

[2]Atlantic Oceanographic and Meteorological Laboratory, NOAA, Miami Florida, USA

[3]Leibniz Institute of Marine Sciences (IFM-GEOMAR), Kiel, Germany

[4]National Center for Atmospheric Research, Boulder, Colorado, USA

[5]Rosenstiel School for Marine and Atmospheric Science, University of Miami, Miami, Florida, USA

Submitted to Variations

May 2011

Corresponding author address: Dr. Sang-Ki Lee, NOAA/AOML, 4301 Rickenbacker Causeway, Miami, FL 33149, USA. E-mail: Sang-Ki.Lee@noaa.gov.

As seen in the extended reconstructed sea surface temperature data (ERSST3; Smith et al. 2008), the North Atlantic sea surface temperature (SST) during the instrumental period (Figure 1a) contains both a secular increase at a rate of ~ 0.4^{o}C per 100yrs during 1901-2010 and a robust multidecadal signal of similar amplitude, known as the Atlantic multidecadal oscillation (AMO; Kerr, 2000). Coupled general circulation models forced by external factors such as greenhouse gases and solar variations do a poor job of reproducing the AMO in the 20th century, suggesting that it must arise instead from internal interactions of the climate system (e.g., Knight, 2009). It has been shown that in an unforced coupled climate model simulation the Atlantic meridional overturning circulation (AMOC) exhibits decadal to multidecadal (15 - 70 yrs) variations and is closely linked both dynamically and statistically to the AMO (e.g., Delworth et al., 1993). However, neither the long-term variations of the AMOC nor the link between the AMOC and AMO has been demonstrated with observations in the 20th century because historical observations of the AMOC are not up to the task.

Contrary to the North Atlantic SST, the South Atlantic SST during the instrumental period (Figure 1b) has increased almost linearly at a rate of ~ 0.9^{o}C per 100yrs during 1901-2010, clearly surpassing the global average of 0.6 ~ 0.7^{o}C per 100yrs. Consistent with this surface trend, recently updated and bias-corrected instrumental records indicate that the heat content of the Atlantic Ocean in the upper 700m has substantially increased during the 1970s – 2000s at a rate (~ 8×10^{22} J per 40yrs) almost matching that of the Pacific Ocean (~ 6×10^{22} J per 40yrs) and Indian Ocean (~ 2×10^{22} J per 40yrs) combined (Levitus et al., 2009), even though the Atlantic Ocean covers less than 20% of the global ocean in surface area. As a candidate mechanism for the differential inter-ocean warming, Lee et al. (2011) pointed out the potential role played by the global overturning circulation. They argued that as the upper ocean warms globally during

the 20th century, the inter-ocean heat transport associated with the global overturning circulation should increase until the deep ocean fully adjusts to the surface warming or the global overturning circulation slows down. Since the Atlantic Ocean is characterized with advective heat convergence, they argued that the Atlantic Ocean should therefore gain extra heat from other oceans. They used a surface-forced global ocean-ice coupled model to test this hypothesis and to further show that the increased AMOC at 30^{o}S, forced by the increased wind stress curl over the region from 50^{o} to 30^{o}S, has contributed greatly to the increased inter-ocean heat transport from the Indian Ocean during the latter half of the 20th century.

To sum up, it appears that the AMOC and the associated meridional ocean heat transport hold the key to our understanding of the observed secular and multidecadal warming of the North and South Atlantic Oceans since the mid-20th century. Therefore, it is vital to reconstruct the history of AMOC and associated meridional ocean heat transport in the 20th century, covering at least one full cycle of the AMO to be able to cleanly distinguish the secular trend from the multidecadal variations. Here, we attempt an ocean model-based reconstruction, which is likely to be our best chance for assessing the history of AMOC in the 20th century because the observed surface flux fields, which constrain ocean-only (or ocean-ice coupled) models, are available on relatively long time scales.

20th Century Reanalysis (20CR)

None of the surface-forced ocean model studies so far has been simulated with the surface forcing prior to the mid-20th century because the surface forcing data, which are typically derived from atmospheric reanalysis products such as NCEP-NCAR reanalysis, are limited to the last 50 - 60 years. Recently, the newly developed NOAA-CIRES 20th Century Reanalysis

(20CR) has been completed (Compo et al., 2010). The 20CR provides the first estimate of global surface momentum, heat and freshwater fluxes spanning the late 19th century and the entire 20th century (1871-2008) at daily temporal and 2^o spatial resolutions.

Model Experiments

The global ocean-ice coupled model of the NCAR Community Climate System Model version 3 (CCSM3) forced with the 20CR is used as the primary tool in this study. The ocean model is a level-coordinate model based on the Parallel Ocean Program (POP), divided into 40 vertical levels. The ice model, the NCAR Community Sea Ice Model version 5, is a dynamic-thermodynamic ice model. Both the ocean and ice models have 320 longitudes and 384 latitudes on a displaced pole grid with a longitudinal resolution of about 1.0 degrees and a variable latitudinal resolution of approximately 0.3 degrees near the equator. See Doney et al. (2007) for more detailed descriptions about the CCSM3 ocean-ice model (CCSM3_POP hereafter).

After the total of 900 years of spin up runs (see Lee et al. (2011) for a detailed description of the spin up runs), three model experiments are performed. In the control experiment (EXP_CTR), the CCSM3_POP is integrated for 1871-2008 using the real-time daily 20CR surface flux fields. The next two experiments are idealized experiments designed to understand the Atlantic Ocean heat content change with and without the influence of the northward heat transport change at 30^oS. The remote ocean warming experiment (EXP_REM) is identical to EXP_CTR except that the surface forcing fields north of 30^oS are from the daily 20CR surface flux fields for the period of 1871-1900 exactly like the spin-up experiment, whereas those south of 30^oS are real time as in EXP_CTR. The Atlantic Ocean warming experiment (EXP_ATL) is also identical to EXP_CTR except that the surface forcing fields south of 30^oS are from the daily

20CR surface flux fields for the period of 1871-1900 as in the spin-up experiment, whereas those north of 30^{o}S are real time as in EXP_CTR. Note that the Atlantic Ocean warms only through anomalous surface warming (i.e., local processes) in EXP_ATL, and only through anomalous northward ocean heat transport at 30^{o}S (i.e., remote processes) in EXP_REM, respectively.

Model Results

Figure 2a shows the simulated North Atlantic Ocean heat content change in the upper 700m in reference to the 1871 - 1900 period obtained from the three model experiments, along with the observed trend of the North Atlantic Ocean heat content during 1969 – 2008. The observed trend is referenced at 1969 in Figure 2 for a better visual comparison with the simulated trends. The simulated North Atlantic Ocean heat content in EXP_CTR increases moderately during the 1930s - 1940s, and then decreases during the 1940s - 1970s, after which it increases substantially much like the AMO from observations (Figure 1a). Between the 1970s and 2000s, it increases by 3 ~ 4×10^{22} J. This large increase is reasonably close to the observed North Atlantic Ocean heat content increase of ~ 5.5×10^{22} J during the same period (Levitus et al., 2009), suggesting that the model experiment (EXP_CTR) reproduces reasonably well the heat budget trend of the North Atlantic Ocean after the 1960s.

If the northward heat transport in the South Atlantic at 30^{o}S is fixed at its 1871-1900 level by considering the fully transient surface fluxes only north of 30^{o}S (EXP_ATL), the simulated North Atlantic Ocean heat content increases during the 1930s - 1940s, and then decreases during the 1940s - 1970s, almost perfectly reproducing that of EXP_CTR prior to the 1970s. However, the North Atlantic Ocean heat content, in this case, increases by only ~ 1×10^{22} J during the 1970s

and 2000s, and thus cannot explain the observed North Atlantic Ocean heat content increase during the same period.

On the other hand, if the northward heat transport in the South Atlantic at 30^{o}S is allowed to vary in real time by considering the fully transient surface fluxes south of 30^{o}S while keeping the surface fluxes over the Atlantic Ocean at their 1871-1900 levels (EXP_REM), the North Atlantic Ocean heat content increases by ~ 2×10^{22} J during the 1970s – 2000s explaining a moderate portion of the observed trend. In this case, however, the multidecadal signal during the 1930s – 1970s, which is clearly simulated in both EXP_CTR and EXP_ATL is completely missing. The absence of this multidecadal signal in EXP_REM and its presence in EXP_ATL clearly suggest that the multidecadal swing in EXP_CTR prior to the 1970s is caused by processes internal to the Atlantic Ocean. During the 1970s – 2000s, on the other hand, remote processes (i.e., increased inter-ocean heat transport from the Indian Ocean; see Lee et al. (2011)) have contributed more to the large increase in the North Atlantic heat content, although internal processes have also contributed.

Figure 2b is the same as Figure 2a, except for the South Atlantic Ocean heat content change. The simulated South Atlantic Ocean heat content in EXP_CTR remains unchanged until the 1960s, after which it increases monotonically, consistent with the similar increase in the South Atlantic SST during the same period from observations (Figure 1b). Between the 1970s and 2000s, it increases by ~ 2×10^{22} J, slightly less than the observed South Atlantic Ocean heat content increase of ~ 2.5×10^{22} J during the same period (Levitus et al., 2009). As in EXP_CTR, the South Atlantic Ocean heat content in EXP_REM is also characterized with a monotonic increase after the 1960s, but with a smaller amplitude of $1 \sim 2 \times 10^{22}$ J during the 1970s – 2000s. In the case of EXP_ATL, however, there is no apparent change in the South Atlantic heat content

throughout the 20th century. These results derived from Figure 2b lead to a conclusion that remote processes mainly drive the South Atlantic Ocean heat content increase during the 1970s - 2000s in EXP_CTR.

Figure 3a shows the time-averaged AMOC during 1979-2008 obtained from EXP_CTR. The simulated maximum strength of the AMOC at 35^{o}N is only 11 Sv (1Sv = 10^{6} $m^{3}s^{-1}$), which is smaller than the observed range of 14 ~ 20Sv. Despite the smaller maximum strength, the overall spatial structure of the simulated AMOC is quite close to that derived from observations (e.g., Lumpkin and Spear, 2007). Figure 3b shows the time series of the simulated AMOC index (maximum overturning stream function) at three different latitudes, namely 30^{o}S, the equator, and 60^{o}N, in reference to the 1871 – 1900 period. It is clear that the AMOC at all three latitudes increase after the 1950s, with the largest amplitude at 30^{o}S, a lesser amplitude at the equator, and the smallest amplitude at 60^{o}N. This suggests that both the North (0^{o} – 60^{o}N) and South (30^{o}S – 0^{o}) Atlantic Oceans are subject to advective heat convergence during the 1960s – 2000s, consistent with the heat content increase in the North and South Atlantic Oceans during the 1970s – 2000s (Figure 2). It appears that more works are needed to understand if and how the AMOC is linked with the multidecadal variations of the North Atlantic Ocean heat content especially prior to the 1960s.

Acknowledgments

This study was motivated and benefited from the AMOC discussion group of the research community at UM/RSMAS and NOAA/AOML. We wish to thank Igor Kamenkovich and all the participants who led the AMOC discussion group during the past year. We acknowledge helpful suggestions from Ping Chang. This work was supported by grants from the National Oceanic and

Atmospheric Administration's Climate Program Office and by grants from the National Science Foundation.

References

Compo, G. P., and collaborators (2011) The twentieth century reanalysis project. *Quarterly J. Roy. Meteorol. Soc.*, **137**, 1-28. doi: 10.1002/qj.776.

Delworth, T., S. Manabe, and R. Stouffer (1993) Interdecadal variations of the thermohaline circulation in a coupled ocean-atmosphere model. *J. Climate*, **6**, 1993–201.

Doney, S. C., Steve Yeager, G. Danabasoglu, W. G. Large, J. C. McWilliams (2007) Mechanisms governing interannual variability of upper-ocean temperature in a global ocean hindcast simulation. *J. Phys. Oceanogr.*, **37**, 1918–1938.

Kerr, R. A. (2000). A North Atlantic climate pacemaker for the centuries. *Science*, **288**, 1984-1986, doi:10.1126/science.288.5473.1984.

Knight, Jeff R. (2009) The Atlantic multidecadal oscillation inferred from the forced climate response in coupled general circulation models. *J. Climate*, **22**, 1610–1625.

Lee S.-K., W. Park, E. van Sebille, C. Wang, D. B. Enfield, S. Yeager, B. P. Kirtman, and M. O. Baringer (2011) What caused the significant increase in Atlantic Ocean heat content since the mid-20th Century? *Geophys. Res. Lett.*, Submitted.

Levitus, S., J. I. Antonov, T. P. Boyer, R. A. Locarnini, H. E. Garcia, and A. V. Mishonov (2009) Global ocean heat content 1955–2008 in light of recently revealed instrumentation problems, *Geophys. Res. Lett.*, **36**, L07608, doi:10.1029/2008GL037155.

Lumpkin, R. and K. Speer (2007) Global ocean meridional overturning. *J. Phys. Oceanogr.*, **37**, 2550-2562.

Smith, T. M., R. W. Reynolds, T. C. Peterson, J. Lawrimore (2008) Improvements to NOAA's historical merged land–ocean surface temperature analysis (1880–2006). *J. Climate*, **21**, 2283–2296, doi: 10.1175/2007JCLI2100.1.

Figure 1. Observed (a) North (0^o – 60^oN) and (b) South Atlantic (30^oS – 0^o) SSTs during the instrumental period, obtained from ERSST3. The green line in each plot is obtained by performing a 11-year running average.

Figure 2. Simulated (a) North and (b) South Atlantic Ocean heat content changes in the upper 700m in reference to 1871-1900 obtained from the three model experiments. The thick black lines in (a) and (b) are the observed trends of the North and South Atlantic Ocean heat content, respectively, reproduced from Levitus et al. (2009).

Figure 3. (a) Time-averaged AMOC during 1979-2008 and (b) 11-year running averaged time series of the simulated AMOC index (maximum overturning stream function) at 30^oS, the equator, and 60^oN in reference to 1871-1900 obtained from EXP_CTR.

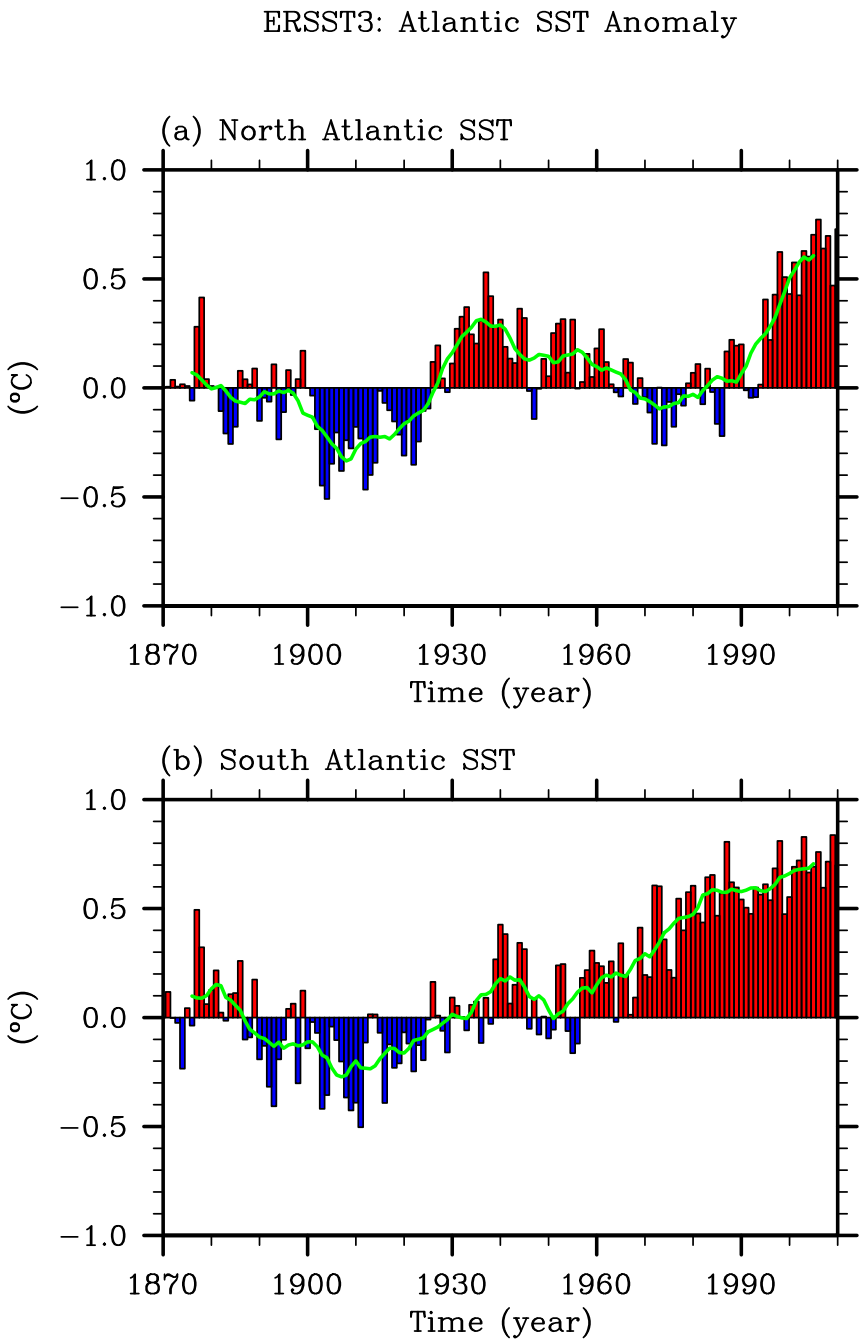

Figure 1. Observed (a) North (0^o – 60^oN) and (b) South Atlantic (30^oS – 0^o) SSTs during the instrumental period, obtained from ERSST3. The green line in each plot is obtained by performing a 11-year running average.

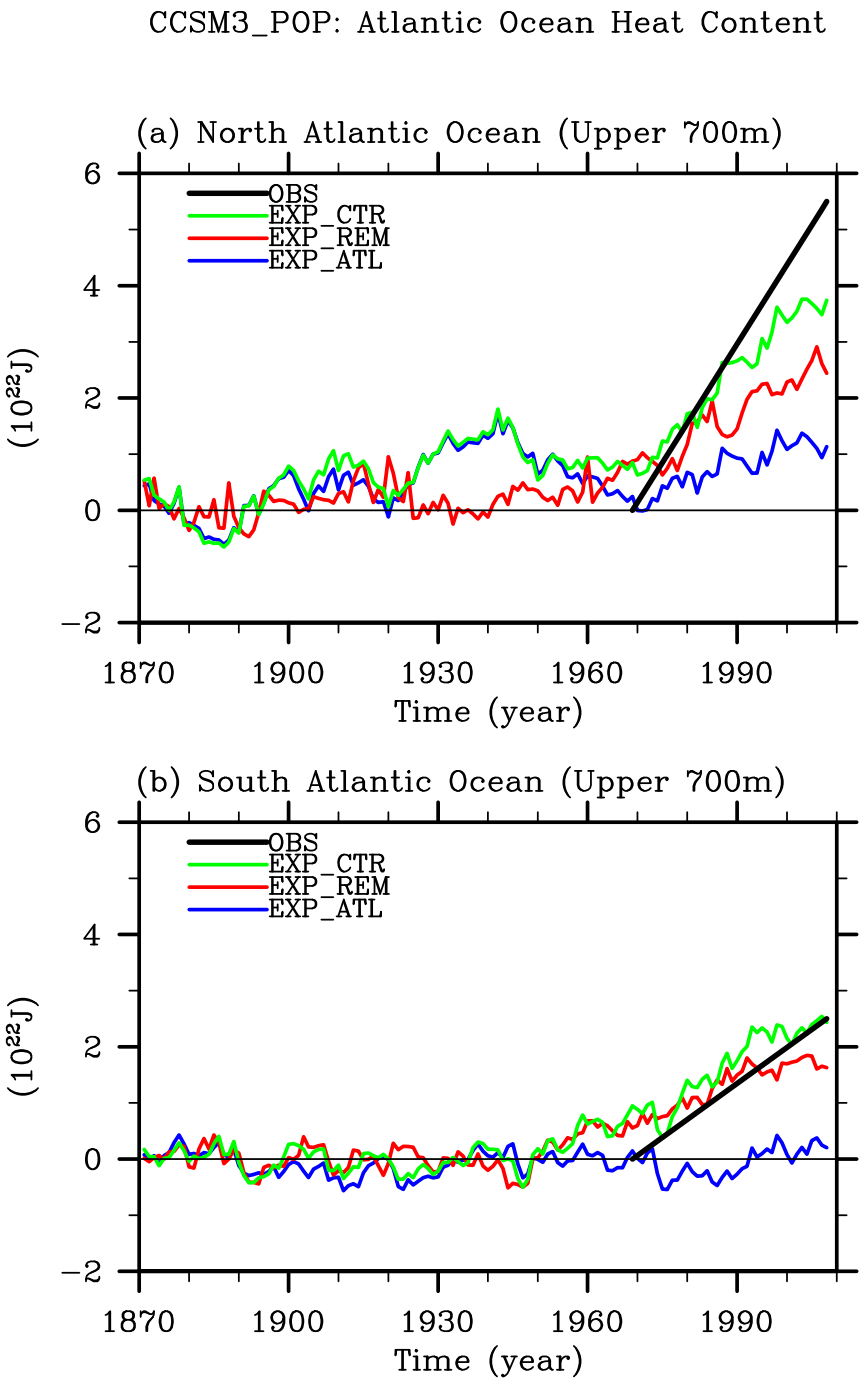

Figure 2. Simulated (a) North and (b) South Atlantic Ocean heat content changes in the upper 700m in reference to 1871-1900 obtained from the three model experiments. The thick black lines in (a) and (b) are the observed trends of the North and South Atlantic Ocean heat content, respectively, reproduced from Levitus et al. (2009).

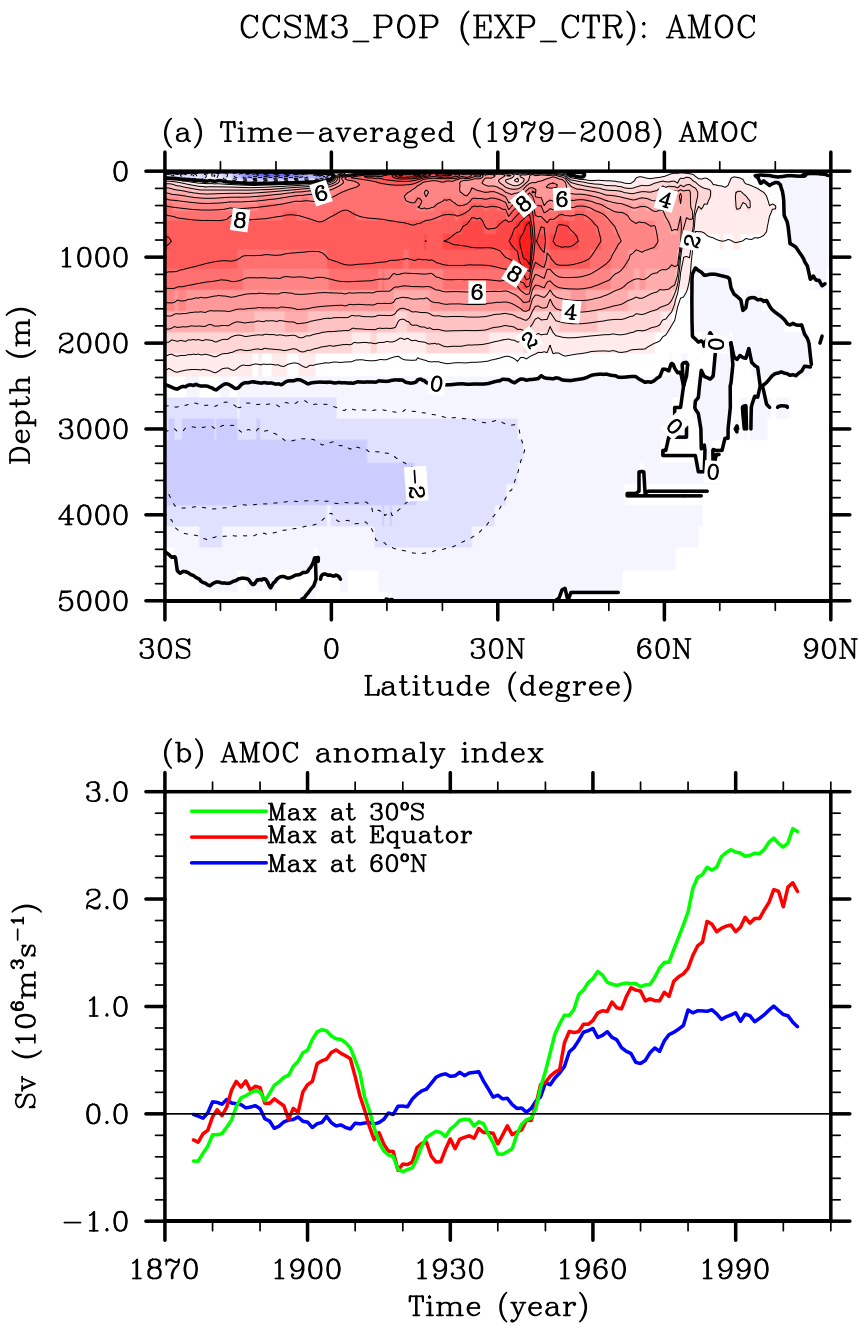

Figure 3. (a) Time-averaged AMOC during 1979-2008 and (b) 11-year running averaged time series of the simulated AMOC index (maximum overturning stream function) at 30°S, the equator, and 60°N in reference to 1871-1900 obtained from EXP_CTR.